frontiers in Behavioral Neuroscience

ORIGINAL RESEARCH
published: 05 June 2018
doi: 10.3389/fnbeh.2018.00115

Rapid ^{18}F-FDG Uptake in Brain of Awake, Behaving Rat and Anesthetized Chicken has Implications for Behavioral PET Studies in Species With High Metabolisms

Maria E. L. Gold[1,2,3], *Mark A. Norell*[1], *Michael Budassi*[4], *Paul Vaska*[4,5,6] *and Daniela Schulz*[7]*

[1] Division of Paleontology, American Museum of Natural History, New York, NY, United States, [2] Department of Anatomical Sciences, Stony Brook University, Stony Brook, NY, United States, [3] Department of Biology, Suffolk University, Boston, MA, United States, [4] Department of Biomedical Engineering, Stony Brook University, Stony Brook, NY, United States, [5] Department of Radiology, Stony Brook University, Stony Brook, NY, United States, [6] Biosciences Department, Brookhaven National Laboratory, Upton, NY, United States, [7] Department of Psychology, Yeditepe University, Istanbul, Turkey

OPEN ACCESS

Edited by:
Ekrem Dere,
Université Pierre et Marie Curie, France

Reviewed by:
Susanne Nikolaus,
Heinrich Heine Universität Düsseldorf, Germany
Owen Chao,
Medical School, University of Minnesota, United States

***Correspondence:**
Daniela Schulz
daniela.schulz@yeditepe.edu.tr

Received: 09 October 2017
Accepted: 18 May 2018
Published: 05 June 2018

Citation:
Gold MEL, Norell MA, Budassi M, Vaska P and Schulz D (2018) Rapid ^{18}F-FDG Uptake in Brain of Awake, Behaving Rat and Anesthetized Chicken has Implications for Behavioral PET Studies in Species With High Metabolisms. Front. Behav. Neurosci. 12:115. doi: 10.3389/fnbeh.2018.00115

Brain-behavior studies using ^{18}F-FDG PET aim to reveal brain regions that become active during behavior. In standard protocols, ^{18}F-FDG is injected, the behavior is executed during 30–60 min of tracer uptake, and then the animal is anesthetized and scanned. Hence, the uptake of ^{18}F-FDG is not itself observed and could, in fact, be complete in very little time. This has implications for behavioral studies because uptake is assumed to reflect concurrent behavior. Here, we utilized a new, miniature PET scanner termed RatCAP to measure uptake simultaneously with behavior. We employed a novel injection protocol in which we administered ^{18}F-FDG (i.v.) four times over two 2 h to allow for repeated measurements and the correlation of changes in uptake and behavioral activity. Furthermore, using standard PET methods, we explored the effects of injection route on uptake time in chickens, a model for avians, for which PET studies are just beginning. We found that in the awake, behaving rat most of the ^{18}F-FDG uptake occurred within minutes and overlapped to a large extent with ^{18}F-FDG data taken from longer uptake periods. By contrast, behavior which occurred within minutes of the ^{18}F-FDG infusion differed markedly from the behavior that occurred during later uptake periods. Accordingly, we found that changes in ^{18}F-FDG uptake in the striatum, motor cortex and cerebellum relative to different reference regions significantly predicted changes in behavioral activity during the scan, if the time bins used for correlation were near the injection times of ^{18}F-FDG. However, when morphine was also injected during the scan, which completely abolished behavioral activity for over 50 min, a large proportion of the variance in behavioral activity was also explained by the uptake data from the entire scan. In anesthetized chickens, tracer uptake was complete in about 80 min with s.c. injection,

but 8 min with i.v. injection. In conclusion, uptake time needs to be taken into account to more accurately correlate PET and behavioral data in mammals and avians. Additionally, RatCAP together with multiple, successive injections of ^{18}F-FDG may be useful to explore changes in uptake over time in relation to changes in behavior.

Keywords: PET, RatCAP, mammal, avian, model species, metabolism

INTRODUCTION

Positron emission tomography (PET), in conjunction with the glucose-analog ^{18}F-fluorodeoxyglucose (^{18}F-FDG), has been used to study brain glucose metabolism in relation to behavior (Kornblum et al., 2000; Myers, 2001; Myers and Hume, 2002; Schiffer et al., 2007). Traditionally, these studies entail the injection of ^{18}F-FDG, production of behavior, anesthesia, and subsequent scanning. However, the development of a new, miniature, portable PET scanner, termed RatCAP, has made scanning animals without anesthesia possible (Schulz et al., 2011). This scanner attaches to the animal's head and is supported by a counter-weighted pendular structure which provides the animal with considerable freedom of motion during the scan (Schulz et al., 2011). The opportunity to simultaneously measure PET activity and behavior can help clarify the correlation between the two data sets.

In PET imaging, uptake time is traditionally measured in dynamic scans in which radioactivity concentrations within brain regions of interest (ROIs) are tracked over time. Early on, ^{18}F-FDG uptake reflects both free tracer in brain tissue and ^{18}F-FDG-6-phosphate, the phosphorylated form of ^{18}F-FDG that becomes trapped inside the brain cell and indicates glucose consumption (Sokoloff et al., 1977; Gallagher et al., 1978; Reivich et al., 1979). But from the first min of uptake up until 2 h following an intravenous (i.v.) injection, virtually all radioactivity in the brain of mice is in the form of ^{18}F-FDG-6-phosphate (Gallagher et al., 1978). Additionally, ^{18}F is mostly cleared from arterial blood, a proxy for free tracer in brain tissue, in less than a minute (Schiffer et al., 2007). This implies that the trapping process that may relate to behavior is potentially complete in a minimum of time. Regardless, PET-behavior studies traditionally allow for 30–60 min of tracer uptake or "trapping" in the awake, behaving state before the animal is anesthetized and scanned (Kornblum et al., 2000; Mirrione et al., 2007; Jang et al., 2009; Shackman et al., 2013; Thompson et al., 2014). The PET data resulting from the images are then correlated with behavior that occurred during "tracer uptake." Because phosphorylated tracer cannot leave the cell until radioactive decay (half-life = 109.7 min), its concentration is relatively stable over time (Gallagher et al., 1978; Schmidt et al., 1996). Thus, the delay from tracer injection to PET imaging an hour later is not problematic for obtaining valid PET data. However, if uptake is actually occurring much faster than the assumed duration of 30–60 min, but 30–60 min worth of behavioral data are correlated with the PET data, then extraneous behavioral data are added or averaged, which could generate misleading results. Hence, uptake time needs to be taken into account to more accurately correlate the PET and behavioral data. In the present study, we have measured uptake time, as defined by the time it takes for the tracer to reach max concentration in the brain of an awake, behaving rat, using RatCAP technology. Moreover, instead of using four rats, we have tested four repetitions in one rat. This repeated-measures approach not only provided confidence in the reliability of our findings, but also allowed for an assessment of transient changes in the brain that might relate to transient changes in the rat's behavior during the PET scan. Thus, the multi-injection protocol might represent a new tool to be used in brain-behavior studies that employ the RatCAP.

Some aspects of biology can affect metabolism and therefore uptake time. An individual animal's metabolism varies depending on its activity, ambient temperature, latitude, food availability, organ, and muscle mass, body size, sex, and age (Mueller and Diamond, 2001; Glazier, 2005; Raichlen et al., 2010; McMurray et al., 2014). In controlled experiments, many of these factors do not significantly vary and so produce no effect. Yet, factors such as behavior, anesthesia, and injection route may affect metabolic rate or the speed at which the tracer reaches the brain and therefore uptake time. These factors have not been studied systematically in all species. Chickens are model animals for birds and non-avian dinosaurs because they are among the more basal extant birds and their biology is well-known (Wagner and Gauthier, 1999; Prum and Dyck, 2003; Welten et al., 2005). Mammals and birds are comparable because of their highly encephalized brains, convergent ecological niches, and high metabolic rates, although differences in glucose metabolism exist between the species. For example, birds have higher levels of glucose in plasma, and the glucose concentration inside the cell is much lower than in plasma whereas it is similar in the mammal (Stevens, 1996). Thus, differences in the uptake of ^{18}F-FDG could be expected between rats and chickens. To date, very few ^{18}F-FDG studies have been conducted in avians. Parrots and eagles have been imaged for diagnostic veterinary purposes (Souza et al., 2010; Jones et al., 2013), crows to study facial recognition (Marzluff et al., 2012; Cross et al., 2013) and starlings to study flight (Gold et al., 2016). In this proof of concept study, we have used chickens to explore the effects of injection route on the uptake of ^{18}F-FDG in forebrain and cerebellum, which represent major divisions in avian neuroanatomy (Balanoff et al., 2013), during wakefulness and under anesthesia. We have tested intravenous (i.v.) and subcutaneous (s.c.) injections because these are recommended routes of drug delivery in birds (Leipold, 1987). Furthermore, we have tested an awake, behaving rat using the RatCAP scanner together with a multi-injection protocol to study uptake times during behavior and to test a new dynamic-like protocol that exploits the potential of the RatCAP scanner.

By injecting ^{18}F-FDG four times, ∼30 min apart, we had the opportunity to study changes in brain uptake that relate to dynamic changes in behavior during the PET scan. We have tested our methods under baseline conditions and following an intervention with morphine. We chose morphine because of its clearly discernible, biphasic effects on motor behavior (Babbini and Davis, 1972; Di Chiara and Imperato, 1988), which we expected to have an observable influence on the PET and behavioral data. We have focused hereby on analyzing ROIs that might link the behavioral activity of the rat to the motor systems of the brain, which include the striatum, motor cortex and cerebellum (Berridge and Whishaw, 1992; Sanes and Donoghue, 2000; Doyon et al., 2003; Kishore et al., 2014). Previously, we could show that ^{11}C-raclopride binding to dopamine D2 receptors in the striatum predicted the behavioral activity of rats wearing the RatCAP (Schulz et al., 2011), but the limited binding profile of the tracer did not allow for correlations with other brain regions. Together, the present studies expand current knowledge by providing an estimate of uptake time of ^{18}F-FDG in two model species and a first demonstration of the relevance of uptake time to behavior in the rat.

METHODS

Subjects

A female adult Long-Evans (LE) rat and a female and two male specific pathogen-free chickens (*Gallus gallus domesticus*) were purchased from Charles River Laboratories (Wilmington, MA). The animals were housed in groups until surgery and individually thereafter. The rat was housed in a standard polycarbonate cage. The chickens were kept in 60 cm high × 1.5 m long × 1.2 m wide pens. The animals were maintained on a 12:12 light:dark cycle (lights on at 7:00 a.m.) with free access to food and water. All procedures were approved by the Institutional Animal Care and Use Committees of Brookhaven National Laboratory, Stony Brook University and the American Museum of Natural History, and were conducted in accordance with the *Guide for the Care and Use of Laboratory Animals*.

Surgeries

Details of the surgical procedures were published in Schulz et al. (2011). In short, jugular vein catheters were implanted for infusion of the radiotracer ^{18}F-FDG. The same procedures were used in the chickens and rat, except that chickens were anesthetized with a ketamine/xylazine mixture (30:3) injected intramuscularly (i.m.), whereas the rat received ketamine/xylazine (10:1) intraperitoneally (i.p). The rat weighed 360 g at the time of surgery. The chickens varied in age (**Table 1**). The jugular vein catheters consisted of 10 cm silastic tubing with one end attached to a back mount cannula connector pedestal (Plastics One, Roanoke, VA). The loose end of the catheter tubing was inserted approximately 2 cm into the jugular vein. A silicone bead on the tubing served as an anchor for sutures. The connector pedestal, which had polyester mesh on the base, was mounted subcutaneously (s.c.) on the back of the animal. To ensure catheter patency, the lines were flushed every 3 days with gentamicin solution (200 μg ml^{-1}). Head surgery was performed only in the rat for later attachment of the RatCAP scanner. Eight anchor screws were attached to the skull for stability of a dental-cement cap. A 2-octyl-cyanoacrylate based tissue adhesive was applied to the skull to affix two screw sockets (7 mm high, 3 mm diameter) onto the midline at bregma and lambda, respectively, for attachment of a magnetic catch that mates with the RatCAP scanner. Dental cement was packed around the sockets except for their openings on the top.

PET Imaging

The rat was moved to the scanner room in its home cage and received a food ration of 50% *ad lib* the night before imaging. It was attached to the RatCAP scanner 1–2 h before the start of the PET scan (see **Figure 1** for study timeline). To this end, the animal was momentarily anesthetized with a bolus of isoflurane gas. A magnetic catch was attached to the screw sockets and the animal's head was placed inside the ring of the scanner, allowing the catch to snap onto a piece on the scanner. A 200-cm-long infusion line made of PE50 tubing was attached to the cannula pedestal on the back of the animal for intravenous (i.v.) administration of the radiotracer. The rat was allowed to wake up and kept in a 50 × 50 cm open field with 30 cm high walls for the duration of the scan (**Figure 2A**). The attachment of the scanner to the rat's head eliminates motion between the head and scanner and, thus, motion artifacts, and with the help of a pendular support structure allows the rat to move around and be active during the scan (Schulz et al., 2011). We conducted two PET scans 19 days apart. In both scans, ^{18}F-FDG (Cardinal Health, Dublin, OH) was administered as a bolus four times ∼30 min apart. The start of the scan coincided with the first injection of ^{18}F-FDG. Injected doses ranged between 300 and 400 μCi. Each dose was given in 200–300 μl of vehicle as per manufacturer and diluted in 0.9% saline to achieve the desired dose of radiation. In the second scan, we also infused (i.v.) 3 mg/kg of morphine diluted in saline (1 ml/kg) using the same PE50 tubing as the one used for the radiotracer. The infusion took place approximately 15 min following the start of the second infusion of ^{18}F-FDG. Following each scan, the RatCAP and magnetic catch were immediately dismounted without the use of anesthesia, and the rat was returned to its home cage. RatCAP data were collected in singles list mode, continually through all injections and the data were monitored to ensure integrity. The lower level discriminator (energy) threshold was 350 keV. The behavior of the rat during the PET scans was filmed using a video camera (SONY, DCR-SR40) placed ca. 1.5 m away from the open field and analyzed *post-hoc*.

The chickens were fasted for at least 45 min before the experiments (see **Figure 3** for study timeline). In the "awake condition" the chickens were allowed to habituate to a pen (100 × 100 cm wide with 45 cm high walls) for 45–60 min (**Figure 2B**). Next, they received 1.4–1.8 mCi of ^{18}F-FDG intravenously (i.v.) via a jugular vein catheter or subcutaneously (s.c.) into a pocket under the right wing near the midpoint of the humerus. The chickens were gently restrained during the injections. They were allowed to move freely inside the pen for approximately 45 min during tracer uptake. The behavior was filmed for later analysis. Anesthesia was then induced with either a mixture of oxygen and

TABLE 1 | Chicken information and imaging combinations for each microPET scan.

Chicken identification number in Figures 9, 10	Sex	Age (weeks)	Approx. Weight (g)	Fasting Time (min)	Anesthetic	Injection Method	Tracer dose (mCi)	Behavioral Conditions
#2	Male	7	540	60	Isoflurane	S.C.	1.44	Anesthetized
#2	Male	18	1,320	At least 45	Isoflurane	I.V.	1.43	Awake
#1	Female	27	1,602	300	0.35 mL Ket/Xy	I.V.	1.8	Anesthetized
#1	Female	29	1,639	200	0.35 mL Ket/Xy	I.V.	1.8	Awake
#3	Male	35	1,690	285	0.35 mL Ket/Xy	S.C.	1.6	Awake

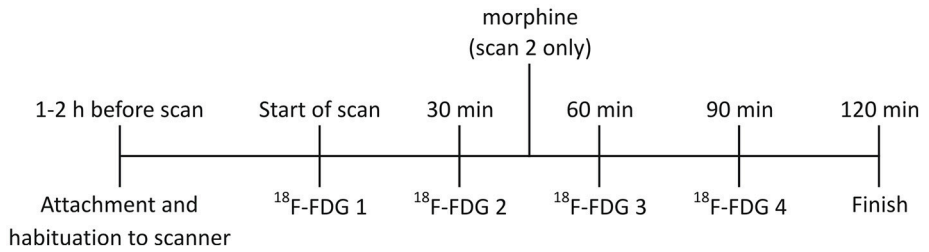

FIGURE 1 | Timeline for RatCAP studies. The rat was attached to the RatCAP 1–2 h before the start of the scan for acclimation to the scanner and the open field. The start of the scan coincided with the first ^{18}F-FDG injection. ^{18}F-FDG was injected 4 times, approximately 30 min apart. In scan 2, morphine (3 mg/kg; i.v.) was also administered approximately 15 min after the second ^{18}F-FDG injection.

isoflurane gas (up to 3%) via nose cone or a ketamine/xylazine injection (100 mg/ml in a 30:3 ratio; i.m.). Glycopyrrolate (0.3 ml; i.m.) was administered to reduce salivation. The animal was fixed on the bed of a microPET R4 scanner (Concorde Microsystems, Knoxville, TN) and the head centered in the field of view (**Figure 2C**). The respiratory rate ranged between 18 and 36 bpm. Body temperature was monitored by a K-type thermometer. A red-light heating lamp was used to maintain body temperature at 38°C ± 1. In the "anesthetized condition" the start of the PET scan coincided with the injection of the tracer, but the scanning procedures were the same as in the "awake condition." These scans were conducted over a 7-month period.

Behavioral Analysis

The behaviors were scored using the manual function of EthoVision software (Noldus, Wageningen, NL). In the rat, we measured "behavioral activity," which included all observable forms of movement, that is, head turns, forward movement, movement of the body without movement of the head, but not the repositioning of the legs while sitting, chewing, and movements related to breathing and sniffing that were not accompanied by locomotion (Schulz et al., 2011). In chickens, we measured movements of the body and head, as well as grooming behavior.

Image Analysis

The RatCAP singles listmode data were processed offline to produce prompt and delayed-coincidence (randoms) sinograms with 47 radial and 24 azimuthal bins. The coincidence window (2τ) was 18 ns. Sinograms were reconstructed using the Maximum Likelihood Expectation Maximization (MLEM) algorithm. The reconstruction included corrections for attenuation, scatter, random coincidences, detector efficiency variations, decay, and deadtime (Southekal et al., 2011). With these methods, the spatial resolution of our images is <2 mm FWHM across the field of view (FOV). Each time frame was reconstructed using 100 iterations, and post-smoothing with a 1.8 mm FWHM Gaussian kernel was applied. The placement of a given ROI within the coordinate space is shown in **Table 2**. The ROIs were determined based on slice thickness (1.07 mm, AP), the RatCAP FOV (∼18 mm minus the first and last slice, AP), the first appearance of the striatum (STR), and a rat atlas (Paxinos and Watson, 2007). The ROIs were drawn on the relevant brain areas using ASIPro software (Siemens). For the striatum (STR), we placed a circle shape (4 pixels) on three successive slices both on the left and the right STR (**Figure 4A**). For the motor cortex (M), a small circle (3 pixels) was placed on the dorsal brain, 1 slice lateral to the midline on either side (**Figure 4B**). For the hippocampus (HIPP), a small circle (3 pixels) was placed 2 slices ventral from the dorsal surface, immediately to the left and right sides of the midline (**Figures 4B,C**). For the cerebellum (CB), a circle (4 pixels) was placed in the center of the dorsal brain (**Figure 4B**). For the amygdala (AMYG), a smaller circle (3 pixels) was placed on two successive slices at the base of the brain, 4–5 slices lateral to the midline on either side, and 4 slices posterior to the most anterior STR (**Figure 4C**). The amygdala ROI included all nuclei of the amygdala but possibly also portions of the piriform cortex. The data from the left and right sides of all relevant ROIs were averaged for analysis. Because the RatCAP scanner is firmly attached to the screw

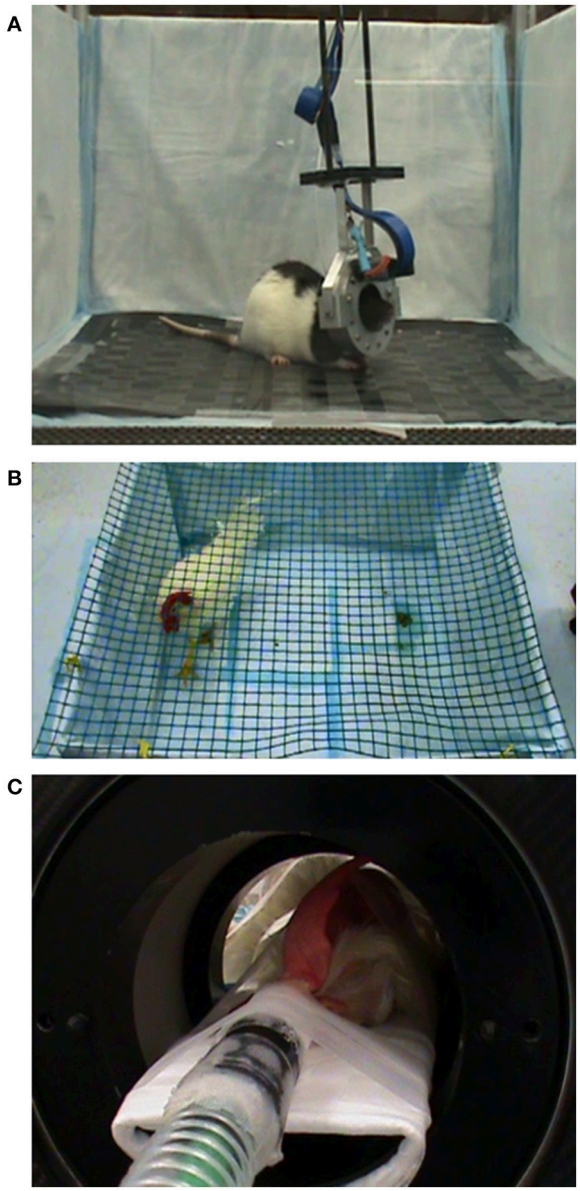

FIGURE 2 | Experimental setup during PET scanning. **(A)** A rat is imaged with the RatCAP scanner while it is awake and spontaneously behaving in an open field. **(B)** A chicken is traversing the pen during uptake of ^{18}F-FDG. **(C)** A chicken under isoflurane anesthesia during PET scanning in the microPET.

sockets on the rat's head and the same rat was scanned twice, we used the same ROI template for both scans. Decay-corrected time-activity curves were generated for 1 min and 20 s time frames.

The chicken imaging data were reconstructed using filtered back projection with frequency cutoff at the Nyquist criterion. Using these methods, the image slice thickness was 1.21 mm (Alexoff et al., 2003). As no digital atlas of a chicken brain is available, ROIs were drawn on two easily visualized divisions of the brain, the forebrain, and cerebellum using ASIPro software (Siemens). In the case of the forebrain, a circle shape (5 pixels) was placed on three successive slices both on the left and the right forebrain (**Figures 5A–C**). The cerebellum ROI (5 pixels) was placed on three slices (along the midline) just posterior to where the forebrain hemispheres transition to the cerebellum (**Figures 5A,C**). The data were binned into 3×20 s, 9×60 s and $n \times 300$ s time frames when the ^{18}F-FDG injection coincided with the start of the scan, and into 300 s time frames when scans were begun after the awake uptake period. The data (mean nCi/cc) were normalized to injected dose/g of animal weight.

Data Analysis

To analyze our rat data, we divided the 120-min-long data sets into 5 min bins (using 20 s frames), because this resulted in a reasonable number of frames to work with in a first exploration of the data. We averaged the PET data and summed the behavioral data for each 5 min bin. To show the rapid uptake of ^{18}F-FDG in the individual ROIs, we calculated the average uptake that occurred within the first 5 min in % of the average uptake that occurred within 25 min of every ^{18}F-FDG injection. To show the progression of uptake across time, we have also calculated the average uptake in the second 5 min, third 5 min, fourth 5 min and fifth 5 min in % of the average uptake across 25 min following every injection. Similar to the PET data analyses, the behavioral activity of the rat was analyzed across successive 5 min time bins in % of the total activity during 25 min following each injection of ^{18}F-FDG. To perform PET-behavior correlations, first we took the ratio of ROI_X/ROI_Y for every 5 min bin to account for residual ^{18}F-FDG from previous injections, where ROI_X was either STR, M or CB, and ROI_Y was a reference region, that is, either a single ROI or a compound ROI, such as the average of M and CB. We have tested various reference regions to study the consistency of results across these regions. To analyze the change in uptake of ^{18}F-FDG in ROI_X relative to ROI_Y across time and to correlate that change with the change in behavioral activity, we took the differences between each of two successive 5 min time bins in line with our previous study (Schulz et al., 2011). We employed the Spearman rank-order correlation to correlate the changes in uptake with the changes in behavioral activity. We performed these correlations for the differences between all 5 min time bins ($n = 23$) as well as the 5 min bins closest to the time of the ^{18}F-FDG injections ($n = 8$). Always three 5 min bins contributed to the difference scores closest to the ^{18}F-FDG injections, the bin preceding the injection and the next two bins, which were then subtracted from each other (bin 2 minus bin 1 and bin 3 minus bin 2), resulting in two difference scores per injection. The injection either coincided with the start of bin 2 or occurred at some point during bin 2. Because the first ^{18}F-FDG injection coincided with the start of the scan and, thus, a bin preceding the injection didn't exist, all three 5 min bins that contributed to the difference scores followed the first injection of ^{18}F-FDG. In correlation analysis, we tested linear functions for significance using the Spearman correlation, but also fitted quadratic and cubic functions to the data in order to detect curvilinear relationships.

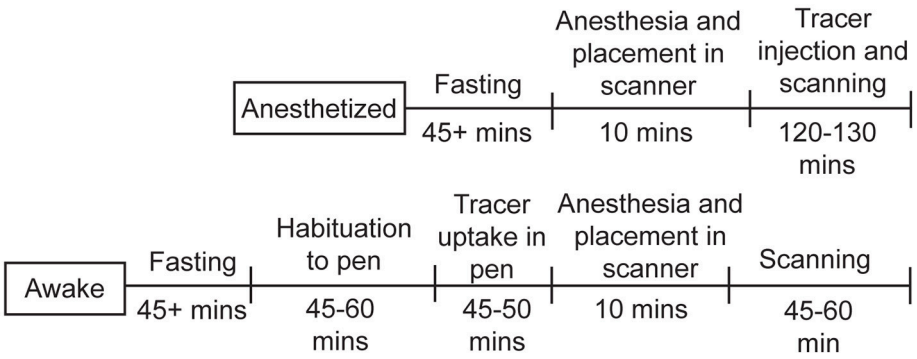

FIGURE 3 | Timeline for chicken studies. For the studies under anesthesia, the chickens were fasted for at least 45 min, then anesthetized, injected with ^{18}F-FDG, and scanned for up to 130 min. For the awake studies, the chickens were fasted for at least 45 min, allowed to habituate to the pen, injected with ^{18}F-FDG and given time for uptake, then anesthetized and scanned for up to 60 min.

TABLE 2 | Location of ROI in coordinate space.

Slices in AP plane	Cumulative mm	AP coordinate of start*	AP coordinate of center*	ROI	ROI
0	1.0766	5.9234	5.3851		
1	2.1532	4.8468	4.3085	M	
2	3.2298	3.7702	3.2319	M	
3	4.3064	2.6936	2.1553	M	STR
4	5.383	1.617	1.0787		STR
5	6.4596	0.5404	0.0021		STR
6	7.5362	−0.5362	−1.0745		
7	8.6128	−1.6128	−2.1511		AMYG
8	9.6894	−2.6894	−3.2277	HIPP	AMYG
9	10.766	−3.766	−4.3043	HIPP	
10	11.8426	−4.8426	−5.3809		
11	12.9192	−5.9192	−6.4575		
12	13.9958	−6.9958	−7.5341		
13	15.0724	−8.0724	−8.6107		
14	16.149	−9.149	−9.6873		
15	17.2256	−10.2256	−10.7639	CB	
16	18.3022	−11.3022	−11.8405	CB	
17	19.3788	−12.3788	−12.9171	CB	
18	20.4554	−13.4554	−13.9937		

According to Paxinos and Watson (2007).

RESULTS

PET-Behavior Studies in Rat Using RatCAP

To show the uptake of ^{18}F-FDG in the behaving rat, we constructed time-activity curves for both scans consisting of 1 min time frames that were averaged for STR, AMYG, HIPP, M, and CB. The scans lasted over 2 h and included four ^{18}F-FDG injections, as indicated by the sudden increases in uptake (**Figure 6A**). It can be seen that most of the tracer was absorbed within the first few min of injection after which uptake appeared to reach a plateau. In fact, when we calculated uptake for each 5 min period in % of the first 25 min following each injection, we found that most of the tracer was taken up in the first 5 min and that very little information was added after that. For all ROIs averaged, 75% of the uptake in scan 1 occurred in the first 5 min following the first injection, and 87, 92, and 94% were taken up in the first 5 min following the second, third and fourth injections, respectively (see **Figure 6B** for data from individual ROIs). Similarly, when morphine was also injected during the scan, 70, 92, 90, and 100% of uptake occurred, on average for all ROIs, in the first 5 min following the first, second, third, and fourth injections of ^{18}F-FDG, respectively (see **Figure 6C** for data from individual ROIs).

Thus, while the PET data appear to be similar for the first 5 min and 25 min following each ^{18}F-FDG injection, the behavior changed markedly across time. To show the levels of behavioral activity across scan time, we summed the activity into 5 min bins and cumulated the bins, so that the display of behavioral activity is represented by a slope increase and the absence of activity by the flat regions in the behavioral response curves (**Figure 6D**). In the first scan, the rat showed progressively less behavioral activity across the first 5 min bins following each ^{18}F-FDG injection (**Figure 6E**). Apart from this regularity, there was no other. The first 5 min of behavioral activity were not predictive of the remaining 5 min bins, not in the first scan (**Figure 6E**) or the second scan (**Figure 6F**). In scan 1, 53% of the behavioral activity that occurred within the first 5 min was also present in the first 25 min following the first ^{18}F-FDG injection. This percentage dropped to 0% with repeated injections. That is, the activity that the animal displayed within the first 25 min occurred at some point past the first 5 min, and thus was not at all represented in the first 5 min when most tracer was taken up in the individual ROIs. Similarly, in the second scan there was an overlap in the data from the first 5 min and 25 min that ranged between 37 and 7% only. This indicates that different results might be obtained when the PET data are correlated with 5 min or 25 min worth of behavior, since the behavioral data contained in these time bins are very different from each other. Thus, correlating the first 5 min of ^{18}F-FDG data with the first 5 min of behavioral

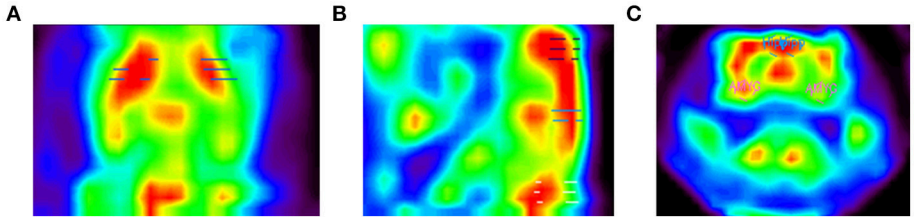

FIGURE 4 | PET images of the rat brain. Depicted are **(A)** a horizontal slice through the brain showing the striatum ROI, **(B)** a sagittal slice showing the motor cortex ROI on top (purple dashes), hippocampus ROI in the center (blue dashes), and cerebellum ROI at the bottom (white dashes), and **(C)** a coronal slice showing the hippocampus (blue circles) and amygdala ROIs (pink circles).

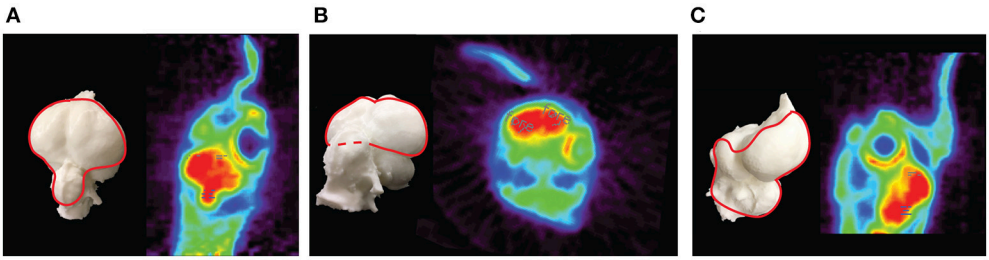

FIGURE 5 | PET images of the chicken brain. Depicted are PET images and corresponding endocasts of the chicken brain. The endocast is a 3-dimensional infilling of the cranial cavity that corresponds to the shape of the brain in a living animal, rotated to be in the same orientation as each PET image. **(A)** A dorsal oblique horizontal slice showing the forebrain (gray dashes) and the cerebellum (blue dashes) ROIs. **(B)** An oblique coronal slice showing the forebrain ROI. **(C)** A sagittal slice showing the forebrain and cerebellum ROIs.

data (but not longer periods) might reduce the confounding effects of subsequent behaviors when correlating the two data sets.

To further explore this idea, we correlated the PET and behavioral data using either all 5 min time frames from the entire scan or only those time frames that captured the data near the injection times. To this end, we took the ratio of uptake in one ROI over uptake in another ROI to account for residuals from previous injections. Next, we calculated the differences between the 5 min time frames on the PET curve and correlated these with the differences in behavioral activity for the same time frames, similar to our approach in our previous study (Schulz et al., 2011). We found that under baseline conditions, changes in uptake in STR, M, and CB relative to various reference regions were predictive of changes in behavioral activity during the scan, but only when the 5 min bins near the times of the ^{18}F-FDG injections were considered, not when all 5 min time bins were included in the analyses (**Table 3**). We fitted both linear and polynomial functions to the data, and in every single case the explained variance was greater (or far greater) when only the time bins near the times of the injections were included for correlation analysis. For example, the inclusion of all 5 min bins did not result in a significant linear correlation between changes in ^{18}F-FDG uptake in STR relative to a compound reference region and changes in behavioral activity ($r = 0.04$, $p = 0.87$; **Figure 7A**), but larger increases in uptake were predictive of larger increases in behavioral activity for the time points near the ^{18}F-FDG injections ($r = 0.69$, $p = 0.06$; **Figure 7B**). Similarly, changes in ^{18}F-FDG uptake in M across scan time were not significantly correlated with changes in behavior when all time bins were included for analysis ($r = 0.03$, $p = 0.88$; **Figure 7C**), but predicted changes in behavior when the time bins near the ^{18}F-FDG injections were included ($r = 0.75$, $p = 0.05$; **Figure 7D**). Moreover, the variability in uptake in CB did not explain a significant proportion of the variance in behavior when all time bins were included ($r = 0.09$, $p = 0.67$; **Figure 7E**), but explained a large proportion of the variance when the time bins near the ^{18}F-FDG injections were included ($r = -0.82$, $p = 0.02$; **Figure 7F**).

In the second scan, in which we tested a morphine intervention, we obtained a somewhat different picture. Although on average, the variance in behavioral activity was still best explained by the variance in uptake in STR, M, and CB when only the 5 min bins near the times of the ^{18}F-FDG injections were included in the analyses, a large proportion of the variance in behavioral activity was also explained by the uptake data from the entire scan (**Table 4**). When we fitted a linear regression line to the data, larger increases in STR uptake relative to a compound reference region predicted significantly larger decreases in behavioral activity when all time bins were included in the analysis ($r = -0.53$, $p = 0.009$; **Figure 8A**), but not when the time bins near the ^{18}F-FDG injections were included ($r = -0.22$, $p = 0.61$), as the latter had a curvilinear association with behavior (**Figure 8B**). Changes in M uptake had positive, linear associations with changes in behavioral

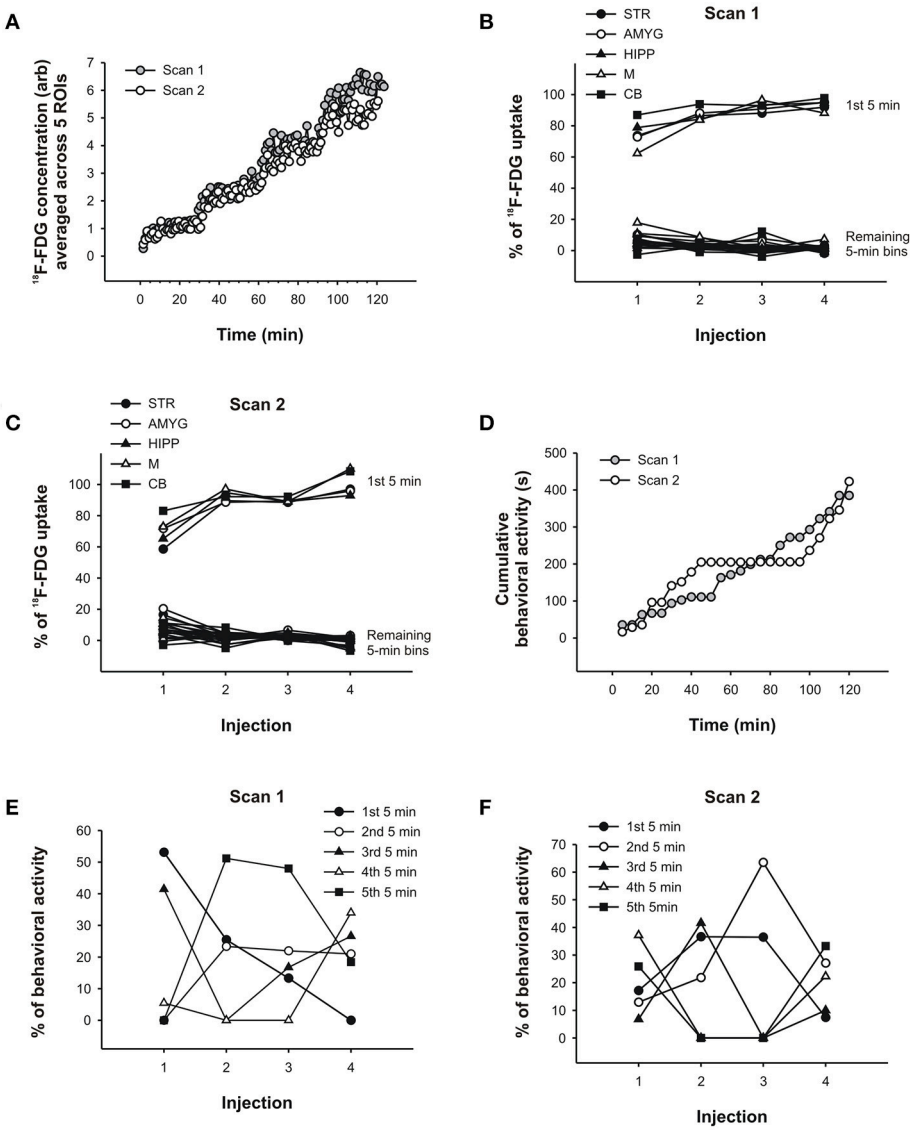

FIGURE 6 | PET data and behavioral analysis for the rat. **(A)** Time-activity curves of scan 1 and scan 2 averaged across 5 ROIs, respectively. ^{18}F-FDG uptake in **(B)** scan 1 and **(C)** scan 2 across successive 5 min time bins in % of the total uptake during 25 min following each injection of ^{18}F-FDG. Most of the uptake occurred within the first 5 min following each injection. These results were similar for all 5 brain regions examined. **(D)** Behavioral activity (s) was summed into 5 min time bins and cumulated, that is, each successive 5 min bin was added to the previous sum. In this way, a slope in the behavioral response curve indicates that the rat displayed activity, whereas flat regions indicate the absence of activity. The prolonged absence of activity starting at 45 min in scan 2 coincides with the injection of morphine. Similar to the PET data analyses in **(B,C)**, the behavioral activity of the rat in scan 1 **(E)** and scan 2 **(F)** was analyzed across successive 5 min time bins in % of the total activity during 25 min following each injection of ^{18}F-FDG. The behavior was distributed across time in fairly unpredictable ways. STR, striatum; AMYG, amygdala; HIPP, hippocampus; M, motor cortex; CB, cerebellum.

activity across the entire scan ($r = 0.59$, $p = 0.003$; **Figure 8C**) and for the time bins near the ^{18}F-FDG injections ($r = 0.77$, $p = 0.03$; **Figure 8D**). By contrast, changes in CB uptake did not predict a significant proportion of the variability in behavioral activity when all time bins were included for analysis ($r = 0.06$, $p = 0.78$; **Figure 8E**), nor did a line provide a good fit for the time bins near the ^{18}F-FDG injections ($r = 0.35$, $p = 0.40$), as these data were best represented by a polynomial (**Figure 8F**).

PET-Behavior Studies in Chickens Using MicroPET

In the anesthetized chicken, a comparison of ^{18}F-FDG uptake after s.c. and i.v. administration revealed that uptake time differed profoundly between these two methods. When injected s.c., the tracer was taken up very slowly over a time period of about 80 min (**Figure 9A**). After that, tracer uptake plateaued. By contrast, i.v. injections of ^{18}F-FDG resulted in rapid uptake and a plateau after approximately 8 min (**Figure 9B**).

TABLE 3 | Changes in uptake in ROI relative to a reference region correlated with changes in behavioral activity across scan 1.

Predict behavioral activity from	Coefficient r		Explained variance (%)			
ROI ratio	Linear		Quadratic		Cubic	
	n = 23 All time bins	*n* = 7-8 Near injection	*n* = 23 All time bins	*n* = 7-8 Near injection	*n* = 23 All time bins	*n* = 7-8 Near injection
STR/						
AMYG	−0.20 (0.37)	**0.79 (0.02)**	11.62	82.20	21.40	93.89
AMYG+HIPP	0.10 (0.67)	**0.67 (0.07)**	1.50	62.81	9.65	63.39
HIPP	0.29 (0.18)	0.48 (0.23)	12.95	52.66	13.42	52.99
M	0.03 (0.89)	0.60 (0.12)	12.00	36.33	37.77	66.68
M+CB	0.11 (0.63)	**0.76 (0.03)**	6.49	62.64	30.86	63.54
CB	0.03 (0.89)	***0.96 (0.0005)***	7.75	*94.05*	24.51	*96.43*
AMYG+HIPP+M+CB	0.04 (0.87)	**0.69 (0.06)**	1.26	60.43	14.32	60.58
Average R^2 for STR (%)	2.14	51.74	7.65	64.45	21.70	71.07
M/						
AMYG	−0.20 (0.37)	*0.32 (0.48)*	6.40	*15.48*	16.42	*20.83*
AMYG+HIPP	−0.03 (0.91)	*0.32 (0.48)*	0.51	*10.37*	9.92	*10.97*
AMYG+HIPP+STR	0.01 (0.96)	*0.18 (0.70)*	0.42	*29.76*	16.32	*77.98*
HIPP	0.22 (0.32)	*0.61 (0.15)*	4.95	*55.61*	27.55	*56.21*
STR+CB	0.001 (0.99)	***0.75 (0.05)***	16.92	*71.6*	17.03	*86.48*
CB	−0.08 (0.73)	***0.89 (0.007)***	11.44	*81.8*	31.42	*82.4*
AMYG+HIPP+STR+CB	0.03 (0.88)	***0.75 (0.05)***	6.61	*78.74*	16.50	*88.27*
Average R^2 for M (%)	1.38	36.09	6.75	49.05	19.31	60.45
CB/						
AMYG	0.005 (0.98)	***−0.93 (0.003)***	2.57	*87.76*	19.20	*88.35*
AMYG+HIPP	0.09 (0.67)	***−0.82 (0.02)***	5.32	*77.04*	30.40	*77.64*
HIPP	0.14 (0.52)	***−0.68 (0.09)***	9.22	*49.49*	25.50	*51.87*
STR+M	0.07 (0.74)	***−0.75 (00.05)***	2.88	*82.82*	28.00	*97.7*
AMYG+HIPP+STR+M	0.09 (0.67)	***−0.82 (0.02)***	5.33	*77.04*	31.49	*77.64*
Average R^2 for CB (%)	0.86	64.69	5.06	74.83	26.92	78.64
Average R^2 for all ROIs (%)	1.46	43.92	6.49	62.78	22.64	70.05

STR, striatum; AMYG, amygdala; HIPP, hippocampus; M, motor cortex; CB, cerebellum. AMYG+HIPP and M+CB, average of two regions; AMYG+HIPP+STR, average of three regions, etc. Results are based on rank-order correlations. Bold, p ≤ 0.09; italic, without outlier. Number in brackets, P-value.

In the "awake scans," we didn't have the opportunity to capture the initial ^{18}F-FDG uptake because the chickens were awake and active in a pen during uptake according to standard PET protocols (and were too large to be fitted with the RatCAP). Following uptake in the awake state, anesthesia and placement in the scanner, we found that tracer uptake after an s.c. injection of ^{18}F-FDG had plateaued at 60 min (**Figure 9A**, awake scan), somewhat faster than the data from the "anesthetized scan." The time-activity curve was flat, indicating very little or slow tracer metabolism under this condition. By contrast, following i.v. injections of ^{18}F-FDG the time-activity curves were decreasing by 60 min of uptake time (**Figure 9B**, awake scans), indicating that not only uptake of ^{18}F-FDG is faster after i.v. administration but also the tracer is removed earlier when the chicken is awake during the uptake. This information is relevant especially when behavioral assessments are to be correlated with ^{18}F-FDG uptake.

We assessed body movement (**Figure 9C**), head movement (**Figure 9D**), and grooming behavior (**Figure 9E**) during each scan. A comparison of the behavior that occurred by 8 min (i.v. uptake time found in the present study) with the behavior that accumulated over 30 min (typical uptake time allowed in PET-behavior studies), revealed important differences. In most cases, the quantity of behavior was more after 30 min compared to 8 min, consistent with the rat data. Moreover, the rank order of chickens performing a particular behavior changed with the assessed time period. For example, considering head movement at 8 min, chicken #1 moved more than #3 which, in turn, moved more than #2. At 30 min, #1 moved more than #2 which, in turn, moved more than #3. Similarly, during the first 8 min, chicken #2 groomed for longer durations than #3 and #1, but over the whole 30 min, the rank order changed to #3 ≥ #2 > #1. Thus, consistent with the rat data, the chicken data suggest that confounding effects in brain-behavior studies can be reduced by accurately matching uptake time of the tracer with the occurrence of behavior for the same time period.

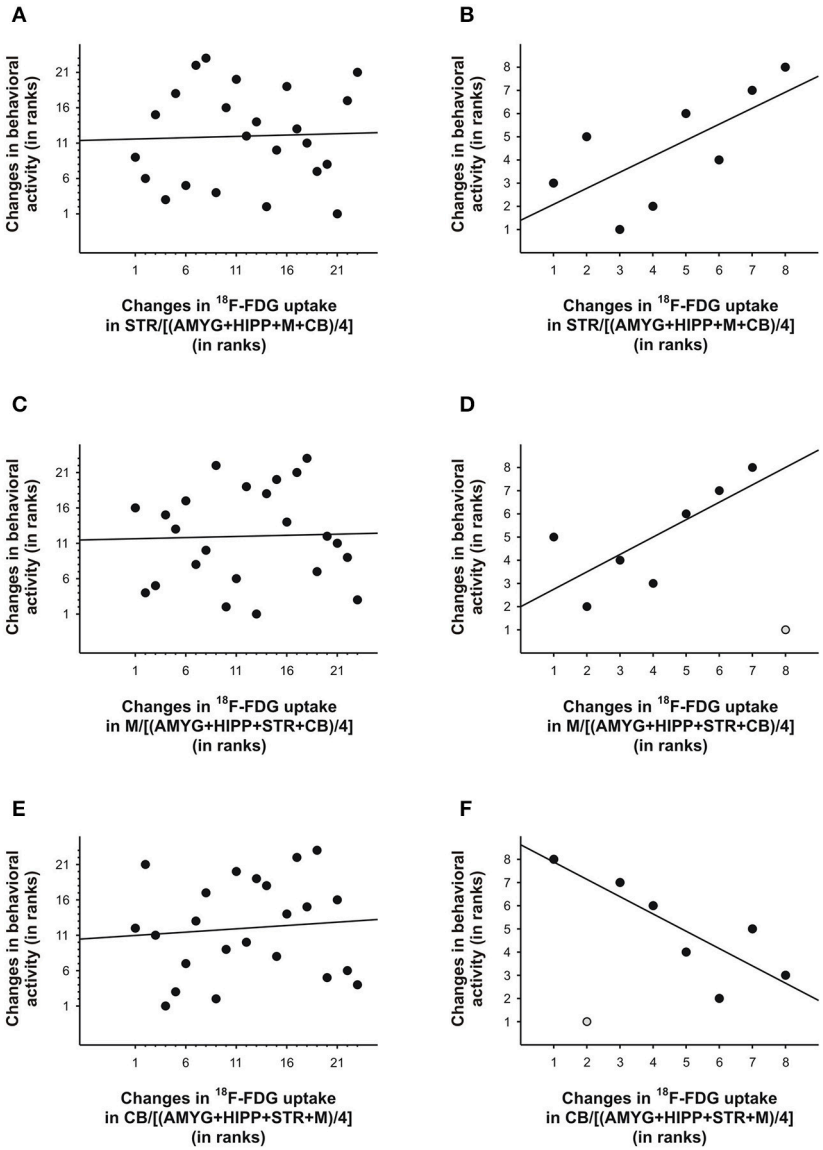

FIGURE 7 | Changes in ^{18}F-FDG uptake correlated with changes in behavioral activity across scan 1 in rat. We correlated changes in ^{18}F-FDG uptake, i.e., differences between successive 5 min time bins, in the **(A,B)** striatum (STR), **(C,D)** motor cortex (M), and **(E,F)** cerebellum (CB) relative to a reference region (the average uptake in a combination of four ROIs) with changes in behavioral activity for the same time frames. When all 5 min time frames ($n = 23$) were included for analysis **(A,C,E),** changes in ^{18}F-FDG uptake did not significantly predict changes in behavioral activity across time. By contrast, for the time frames ($n = 7$–8) near the times of the ^{18}F-FDG injections **(B, D, F),** changes in uptake in STR, M, and CB explained a large proportion of the variance in behavioral activity. The data are represented as ranks. Rank 1 indicates the largest decrease, whereas the highest rank indicates the largest increase between any of two successive 5-min-long time frames. When an outlier (light gray) was present **(D, F)**, the regression line was fitted to the remaining data.

DISCUSSION

In summary, we found that in the awake, behaving rat most of the ^{18}F-FDG uptake occurred within minutes and overlapped to a large extent with ^{18}F-FDG data taken from longer uptake periods. By contrast, behavior which occurred within minutes of the ^{18}F-FDG infusion differed markedly from the behavior that occurred during later uptake periods. Accordingly, we found that changes in ^{18}F-FDG uptake in STR, M, and CB relative to different reference regions significantly predicted changes in behavioral activity during the scan, if the time bins used for correlation were near the injection times of ^{18}F-FDG. However, when morphine was also injected during the scan, which completely abolished behavioral activity for a prolonged period of time, a large proportion of the variance in behavioral activity was also explained by the uptake data from the entire scan. In chickens, uptake time differed profoundly as a function of injection route. Not only uptake of ^{18}F-FDG was faster after i.v. compared

TABLE 4 | Changes in uptake in ROI relative to a reference region correlated with changes in behavioral activity across scan 2.

Predict behavioral activity from	Coefficient r		Explained variance (%)			
ROI ratio	Linear		Quadratic		Cubic	
	$n = 23$ All time bins	$n = 8$ Near injection	$n = 23$ All time bins	$n = 8$ Near injection	$n = 23$ All time bins	$n = 8$ Near injection
STR/						
AMYG	−0.20 (0.35)	−0.43 (0.29)	4.34	22.73	6.43	52.39
AMYG+HIPP	**−0.39 (0.07)**	**−0.65 (0.08)**	16.44	44.25	17.16	44.33
HIPP	**−0.49 (0.02)**	−0.29 (0.49)	24.13	15.20	25.85	18.16
M	**−0.63 (0.001)**	−0.61 (0.11)	42.61	40.12	43.11	40.13
M+CB	−0.07 (0.76)	0.30 (0.47)	9.86	4.34	12.77	46.36
CB	0.27 (0.22)	0.61 (0.11)	7.25	61.42	11.49	62.00
AMYG+HIPP+M+CB	**−0.53 (0.009)**	−0.22 (0.61)	35.87	4.78	35.94	48.23
Average R^2 for STR (%)	16.97	22.49	20.07	27.55	21.82	44.51
M/						
AMYG	**0.51 (0.01)**	0.34 (0.42)	26.48	14.06	26.61	18.47
AMYG+HIPP	**0.53 (0.009)**	0.48 (0.23)	29.25	24.38	29.41	25.30
AMYG+HIPP+STR	**0.57 (0.005)**	0.54 (0.17)	36.57	30.48	36.59	36.18
HIPP	**0.64 (0.001)**	**0.72 (0.05)**	45.82	57.37	45.85	90.23
STR+CB	**0.58 (0.004)**	**0.74 (0.04)**	34.18	82.90	37.82	96.08
CB	**0.53 (0.01)**	0.61 (0.11)	28.28	61.42	28.71	62.00
AMYG+HIPP+STR+CB	**0.59 (0.003)**	**0.77 (0.03)**	38.41	73.44	38.66	85.27
Average R^2 for M (%)	32.01	38.12	34.14	49.15	34.81	59.08
CB/						
AMYG	0.17 (0.45)	0.37 (0.37)	7.13	46.83	12.06	59.33
AMYG+HIPP	0.13 (0.55)	0.37 (0.37)	6.35	46.83	14.70	59.33
HIPP	0.04 (0.86)	0.35 (0.40)	8.53	45.11	17.65	61.99
STR+M	0.03 (0.88)	0.35 (0.40)	14.21	45.11	16.84	61.99
AMYG+HIPP+STR+M	0.06 (0.78)	0.35 (0.40)	8.89	45.11	16.67	61.99
Average R^2 for CB (%)	1.04	12.60	9.02	45.80	15.58	60.93
Average R^2 for all ROIs (%)	16.59	24.40	21.08	40.83	24.07	54.84

STR, striatum; AMYG, amygdala; HIPP, hippocampus; M, motor cortex; CB, cerebellum. AMYG+HIPP and M+CB, average of two regions; AMYG+HIPP+STR, average of three regions, etc. Results are based on rank-order correlations. Bold, $p \leq 0.08$. Number in brackets, P-value.

to s.c. administration but also tracer removal occurred earlier in the awake, behaving chicken. Consistent with the rat data, the behavior of chickens changed markedly over the assessed time period, suggesting that random error could be reduced by accurately matching uptake time of ^{18}F-FDG with the occurrence of behavior for the same time period.

In PET studies, behavior is correlated to a certain pattern of brain activity. ^{18}F-FDG is a glucose analog so it is taken in by active neurons that need fuel. Hence, the behavior in question must occur during the period of tracer uptake because then the resulting images will show the active areas of the brain during the desired behavior. Standard PET scanning usually allows for 30–60 min of ^{18}F-FDG uptake in mammals before the induction of anesthesia and PET scanning. This uptake period is then used for the summation of all behavioral data and correlation with the PET data (Kornblum et al., 2000; Mirrione et al., 2007; Jang et al., 2009; Shackman et al., 2013; Thompson et al., 2014). It has not been previously possible to measure the actual uptake time of ^{18}F-FDG in an awake, behaving rat because small animal PET scanners required complete stillness to image the animal without motion artifacts. The invention of the RatCAP scanner that attaches to the animal's head has opened the door for simultaneous imaging and behavioral observation (Schulz et al., 2011; Gold et al., 2016). Using this device, the present study showed that most of the ^{18}F-FDG uptake in an awake, behaving rat occurred within 5 min or less. This insight is important to acknowledge if random error in brain-behavior correlations is to be reduced.

Firstly, when ^{18}F-FDG data are treated in isolation, averaging more rather than less data is meaningful to reduce error related to photon counting statistics, also considering the relative consistency of the data across time. In this study, the data from the first 5 min and first 25 min overlapped to a large extent, ranging from ∼60 to 80% for five different ROIs after the first ^{18}F-FDG injection to over 90% following repeated injections. Thus, although the initial uptake is most informative, the degree of uptake can be inferred from later time points due to the stability

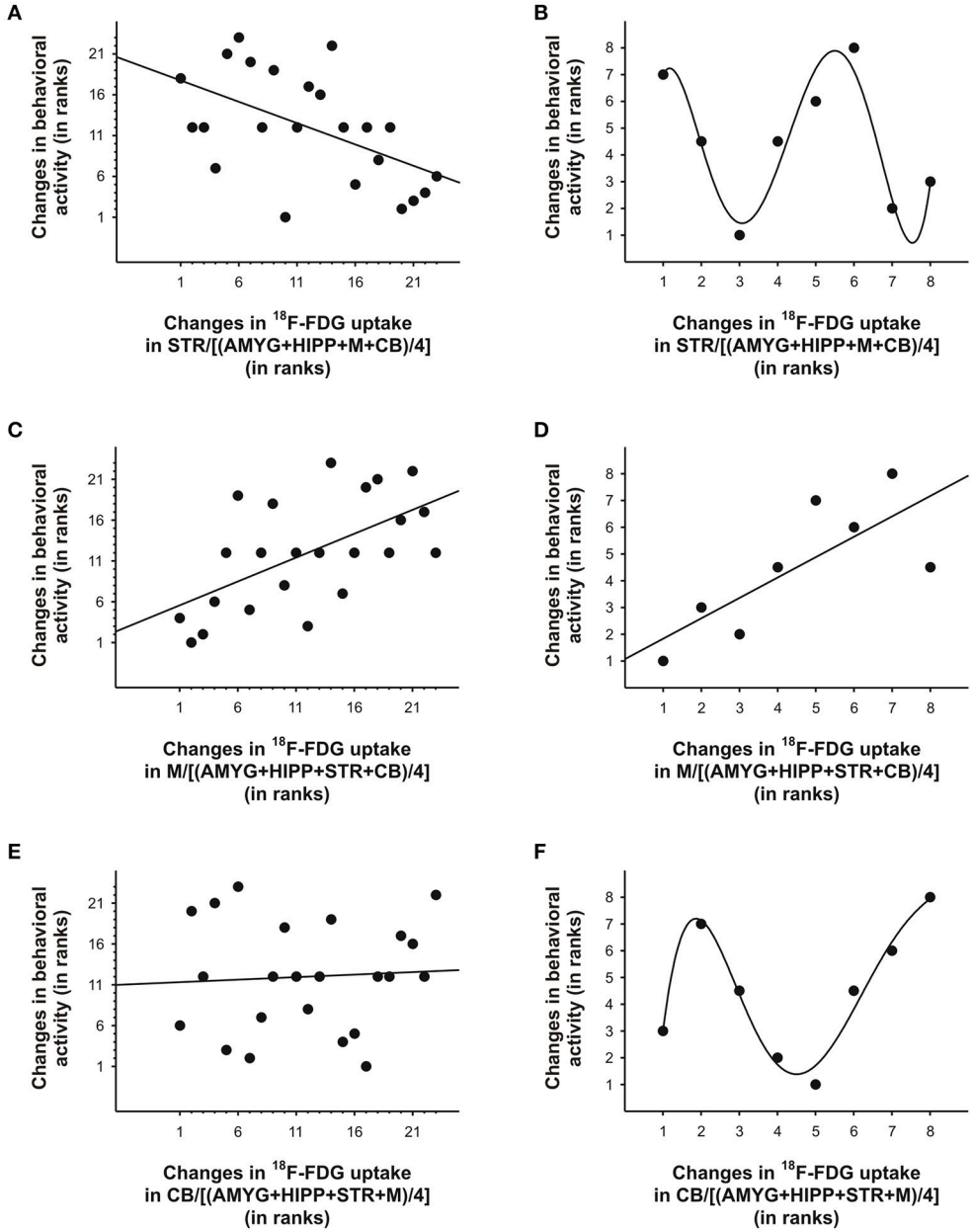

FIGURE 8 | Changes in ^{18}F-FDG uptake correlated with changes in behavioral activity across scan 2 in rat. We correlated changes in ^{18}F-FDG uptake, i.e., differences between successive 5 min time bins, in the **(A, B)** striatum (STR), **(C, D)** motor cortex (M), and **(E, F)** cerebellum (CB) relative to a reference region (the average uptake in a combination of four ROIs) with changes in behavioral activity for the same time frames. When all 5 min time frames ($n = 23$) were included for analysis **(A, C, E),** changes in ^{18}F-FDG uptake in the STR and M, but not CB, significantly predicted changes in behavioral activity across time. When only the time frames ($n = 7$-8) near the ^{18}F-FDG injections **(B, D, F)** were included for analyses, a linear function could be used to predict changes in behavioral activity from changes in uptake in M **(D)**, but polynomial functions provided the best fit for the data from STR **(B)** and CB **(F)**. For illustration, we fitted a quintic polynomial to the data **(B, F)**. The data are represented as ranks. Rank 1 indicates the largest decrease, whereas the highest rank indicates the largest increase between any of two successive 5-min-long time frames.

of the tracer once it is taken up. This stability is the result of a unique property of ^{18}F-FDG which, unlike glucose, becomes trapped inside the cell as ^{18}F-FDG-6-phosphate until decay of the isotope (Sokoloff et al., 1977; Gallagher et al., 1978). This metabolic trapping does not occur in all tissues equally but is highly evident in the brain and heart of mammals (Gallagher et al., 1978).

By contrast, behavior is dynamic and variable across short periods of time. This short latency for change is a challenge for PET studies which collect relatively static data across longer

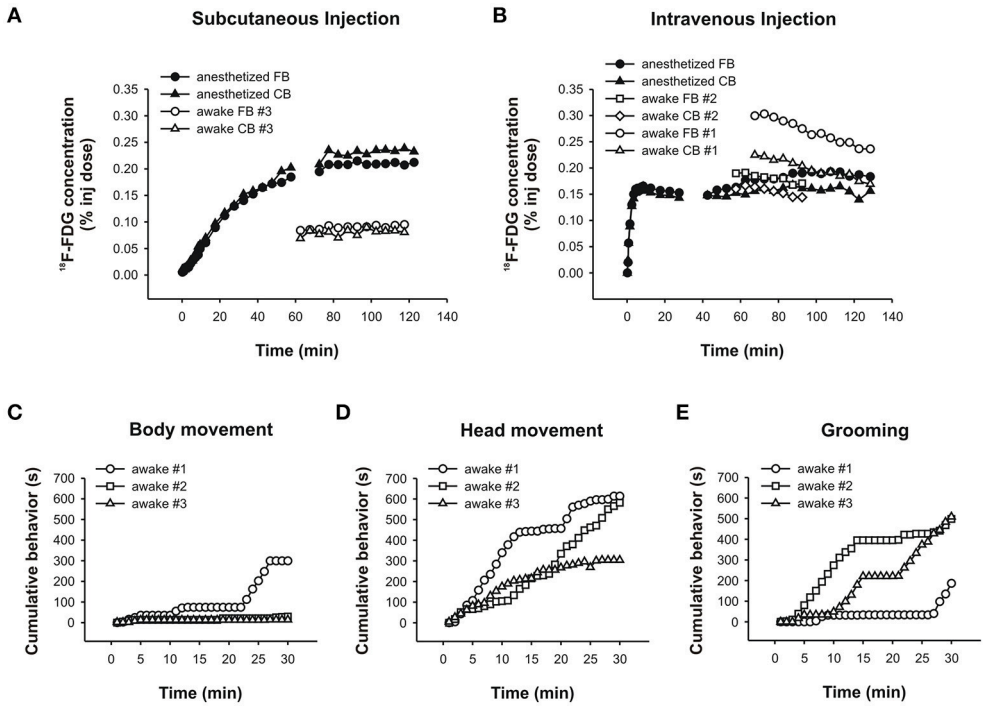

FIGURE 9 | PET data and behavioral analyses for the chicken. Time-activity curves for the chicken following a **(A)** subcutaneous injection of ^{18}F-FDG showing an anesthetized (black symbols) and an awake (white symbols) uptake study. Circles and triangles show uptake in the forebrain and cerebellum, respectively. **(B)** Intravenous injection of ^{18}F-FDG showing an anesthetized (black symbols) and two awake (white symbols) uptake experiments. Circles and squares show uptake in the forebrain, and triangles and diamonds show uptake in the cerebellum. The time-activity curves for the anesthetized animal is shown in two parts due to subject motion midway through the scan. Durations (s) of **(C)** body movement, **(D)** head movement and **(E)** grooming were summed for each 1 min time bin and cumulated. The rank order of chickens spending time engaging in each behavior changed when the initial 5–10 min were considered versus the entire 30 min of ^{18}F-FDG uptake.

periods of time but aim to reflect behavior in brain images in sensitive ways. In our example, the overlap in behavioral activity the rat showed in the first 5 min and 25 min after each ^{18}F-FDG injection ranged from ∼50 to 0%, indicating that the behavior can change markedly across short periods of time. Typically, behavioral activity will accumulate over time, and more behavior will be displayed over longer compared to shorter periods of time, consistent with our data. On the other hand, rats are also known to become less active over time in response to an increase in familiarity of the environment (Berlyne, 1955, 1966). Consistent with this notion, we observed that under baseline conditions the rat's activity decreased across the first 5 min bins following each ^{18}F-FDG infusion, perhaps indicative of habituation. Other than this regularity, however, and the fact that morphine abolished all behavioral activity for about an hour of scan time, activity levels were variable.

We found that changes in ^{18}F-FDG uptake were correlated with changes in behavioral activity during the scan, which suggests that our behavioral neuroimaging approach can be used with reversible (Schulz et al., 2011) and irreversible PET tracers. Specifically, we found that under baseline conditions changes in ^{18}F-FDG uptake in STR, M, and CB, as defined by differences in average ^{18}F-FDG concentrations between each of two successive 5 min intervals, were predictive of changes in spontaneous behavioral activity, if the time bins captured the first ∼10 min following an ^{18}F-FDG injection. This finding corroborates the conclusion that most of the information is contained where most of the uptake occurs and, thus, that uptake times of ^{18}F-FDG should match the time periods used for behavioral analysis if random error in PET-behavior correlations is to be reduced. On the other hand, when the rat was injected with morphine during the scan, a slightly different picture emerged. On average, the variance in behavioral activity was still best explained by the variance in uptake in STR, M, and CB when only the time bins near the ^{18}F-FDG injections were included in the analyses. However, a large proportion of the variance in behavioral activity was also explained by the uptake data from the entire scan, though this was the case for STR and M, but not CB. Perhaps the morphine injection resulted in a separation of data categories, such as pre- and post-injection levels of behavioral activity and activity absenteeism in the middle of the scan, which somehow produced the correlations artificially, although we do not have evidence for that. Perhaps the behavior was constant or predictable enough across time to produce meaningful correlations with the uptake data from the entire scan. Future RatCAP research will need to delineate the conditions that produce such differences between scans.

We chose to focus our analyses on STR, M, and CB because these regions are well known to mediate motor functions (Albin et al., 1989; Berridge and Whishaw, 1992; Sanes and Donoghue, 2000; Doyon et al., 2003; Kishore et al., 2014), and in a previous study we found a correlation between changes in dopamine D2 receptor binding in STR and changes in behavioral activity in a rat wearing the RatCAP (Schulz et al., 2011). We have tested different ROIs, single, and combination ROIs, as reference regions to account for residual ^{18}F-FDG from previous injections. While the choice of the amygdala and hippocampus were arbitrary, these regions are non-motor regions known to mediate emotional and contextual memories (Morris et al., 1982; LeDoux, 1993), that we'd expect to have a relatively slow time course compared to the rapid dynamics of motor activity. On the other hand, motor functions, such as skill learning and motor adaptation, also involve memory processes. Indeed, given some variability, we mostly found consistent results with motor and non-motor ROIs as reference regions.

Interestingly, we found positive correlations between changes in STR uptake and behavioral activity under baseline conditions but negative correlations between the data sets when morphine was also administered during the scan. While ^{18}F-FDG uptake in the STR is not specific to one cell type, the large majority of cell bodies in this region are GABAergic medium spiny neurons (MSNs), which are an important component of the striatal output pathways that organize motor behavior (Kita and Kitai, 1988; Albin et al., 1989; Gerfen et al., 1990). These neurons contain dopamine receptors (Gerfen et al., 1990), which mediate a net increase in movement when activated by dopamine (Wichmann and DeLong, 2010). Importantly, these neurons also contain mu-opioid receptors (MOR) to which morphine binds (Wang et al., 1996, 1997). In fact, a large number of MORs are located on the dendrites of MSNs that receive dopaminergic terminals from the substantia nigra (Wang et al., 1997), indicating that morphine could modulate the post-synaptic effects of dopamine receptor binding. A small number of MORs are also located on axon terminals, but not dopaminergic terminals, which suggests that presynaptic MORs on corticostriatal afferents modulate glutamatergic input into the striatum (Wang et al., 1997). Correlations between changes in M uptake and behavioral activity were positive throughout our study, which suggests that the modulation through morphine occurred downstream from M but possibly via an effect of presynaptic MORs on striatal neurons. MOR agonists given systemically increase dopamine release in STR, which was found to correlate with a biphasic effect on behavior at higher doses (Babbini and Davis, 1972; Di Chiara and Imperato, 1988). Consistent with these findings, we also observed that morphine completely suppressed behavioral activity for about an hour, which was followed by hyperactivity as indicated by the steep upward slope in the late part of the rat's cumulative response curve. While glucose uptake is not confined to specific subcellular domains such as cell bodies (Maher, 1995), our data suggest that morphine modulated the functioning of MSNs in STR, thereby impacting the associations between ^{18}F-FDG uptake in STR and behavior. MORs appear to be absent in the rat cerebellum (Schadrack et al., 1999), so that the modulation from positive correlations with CB under baseline conditions to curvilinear correlations when morphine was injected during the scan must be attributed to indirect effects on the cerebellum, possibly via descending pathways originating from the motor cortex (Kishore et al., 2014).

The dynamic-like injection protocol used with RatCAP in the present study allowed for a first demonstration of a link between changes in brain uptake of ^{18}F-FDG and changes in behavior that occurred over the course of the PET scan. The present method is a derivative of the method we have used with ^{11}C-raclopride in our earlier study (Schulz et al., 2011), with the difference that ^{18}F-FDG is not a reversible tracer like ^{11}C-raclopride. In both cases is the repeated administration of tracer necessary to be able to obtain neurochemical measures that are capable of reflecting short-term behavioral changes. Such changes can only be assessed with a tool, such as RatCAP, which allows for the simultaneous measurement of brain and behavioral processes. While we chose to inject ^{18}F-FDG every 30 min in the present study, the relatively short uptake times suggest that shorter injection intervals could also be tested in the future to allow for an assessment of even shorter dynamics. It should be pointed out that the cabling and data acquisition systems that sit on top of the pendular support structure limit the animal's movements. For example, rearings, a vertical form of exploratory behavior, and grooming behavior are not or very rarely observed. Thus, it will be important in future RatCAP research to increase mobility more and/or to construct behavioral paradigms that allow for greater variations in behavior.

The use of PET in avians is in its infancy, and has been used for veterinary diagnostics (Souza et al., 2010; Jones et al., 2013) and very few behavioral studies (Marzluff et al., 2012; Cross et al., 2013; Gold et al., 2016). The RatCAP provides an ideal way to study behaviors in birds, and while we were able to use it successfully in starlings (Gold et al., 2016), the size of the chickens and the presence of a waddle and comb impeded the use of the RatCAP. Inspired by the rapid uptake we observed in rats, and the comparability between mammals and avians, we were interested to explore uptake times in chickens.

We found several factors affecting uptake time in chickens. One of these factors was injection route. Here, anesthetized chickens were injected via s.c. and i.v. routes. The s.c. injection resulted in a long uptake time, approximately 80 min. However, the i.v. injection resulted in approximately 8 min of uptake time. This suggests that uptake period decreases in relation to increasing directness of the injection route to the circulatory system. Most previous avian PET studies have used i.v. injection routes either through the jugular (Souza et al., 2010) or basilica (Jones et al., 2013) veins, though Marzluff et al. (2012) and Cross et al. (2013) used an i.p. injection in their behavioral studies. Even though birds have a peritoneal cavity, injection into this cavity is not recommended due to the presence of air sacs scattered throughout the abdomen (Fowler, 2007; Fair et al., 2010). Muscles provide a secure injection route for most drugs in birds without endangering the air sac system. By contrast, i.m., and s.c. injections are not usually used in rodent PET studies. However, one study found that ^{18}F-FDG injected s.c. resulted in low levels of uptake in lymph nodes (Wahl et al., 1990). In rats, i.v. injections are preferred although i.p. injections are also

sometimes used. One study in anesthetized rats demonstrated that ^{18}F-FDG concentrations peaked after 30 min using an i.p. route, but peaked in less than 10 min using an i.v. route (Schiffer et al., 2007). Researchers could make use of this knowledge by choosing an injection route that accommodates behaviors of different durations. This would insure that the behavior is fully captured during the uptake time.

We have measured three behaviors in chickens while in a pen—body movement, head movement, and grooming. Overall, the activity levels were higher if cumulated over longer than shorter periods of time, consistent with the rat data. Importantly, the chickens differed in the durations that they displayed each behavior across time, at times converging and at times diverging in the amount of performance. In the case of head movements and grooming behavior, the rank order of chickens performing each behavior was different for the first 8 min of ^{18}F-FDG uptake and the first 30 min. Thus, depending on the time period used to assess the behavior of interest for correlation with the PET data, different results would be obtained. Future avian research might benefit from comparing shorter with longer time periods used for behavioral assessments that are adjusted to uptake time and, thus, injection route for correlation with the PET data.

While we had considerable variability in the protocols of our chicken studies, the differences in the fasting protocols were unlikely to have affected glucose uptake and, thus, ^{18}F-FDG concentrations in the tissues. Birds, including chickens, show a remarkable stability in blood glucose levels even after days of fasting (Belo et al., 1976; Stevens, 1996). Less is known about the influence of different anesthetics on PET imaging in birds. The few studies that have been conducted to date, have used isoflurane anesthesia (Souza et al., 2010; Marzluff et al., 2012; Cross et al., 2013; Jones et al., 2013). We have also tested isoflurane in the chickens first, but found it to be unsuitable due to respiratory ailments even after injection of glycopyrrolate which is commonly used to reduce salivation. On the other hand, the i.m. administration of a ketamine/xylazine mixture presented a workable solution. The impact of the use of different anesthetics as well as other factors, such as age and sex, on the uptake of ^{18}F-FDG in birds remains to be illuminated in future studies.

In the few chickens we have studied, we observed an increase in ^{18}F-FDG uptake over time or, depending on the ROI, stable concentrations in anesthetized chickens but a marked decrease in ^{18}F-FDG concentration following i.v. infusions in the awake state. An explanation of these observations will require some speculation. In birds, unlike mammals, the cell membrane is much less permeable to glucose, and small amounts of glucose are taken up relative to high extracellular concentrations. The uptake increases, however, in the presence of nucleosides like adenosine, at least in red blood cells (Stevens, 1996). Adenosine has many functions, but its increase in the brain is associated with low metabolic states, such as sleepiness and anesthesia (Huston et al., 1996; Gettys et al., 2013). Thus, perhaps the increase in ^{18}F-FDG uptake in anesthetized chickens was due to an accumulation of adenosine or other carriers in tissue that were not present in the awake state. Nevertheless, ^{18}F-FDG concentrations in the chickens were fairly stable following the initial uptake. By contrast, in the avian *Sturnus vulgaris* (Common starlings) we have observed a very fast washout of ^{18}F-FDG that we prevented by administration of insulin (Gold et al., 2016). Marzluff et al. (2012) also recorded a very fast washout of ^{18}F-FDG in crows.

Imaging birds with PET scanning began only recently outside of the veterinary field, primarily to provide a healthy comparison to sick animals (Souza et al., 2010; Jones et al., 2013). Of the many birds that are kept as pets or in zoos, only Hispaniolan parrots (Souza et al., 2010) and bald eagles (Jones et al., 2013) have been examined with ^{18}F-FDG. These studies analyzed tracer uptake in a variety of organs, but did not study how differences in injection route changes uptake rates. One other study evaluated the activity in the brain of crows while viewing different human faces (Marzluff et al., 2012). More recently, we have studied starlings and found that the uptake time following an i.v. injection of ^{18}F-FDG was 3–4 min in the awake state (Gold et al., 2016). The present study expands the taxonomic sampling of birds using PET. These data can be used as a comparison to sick animals or as a baseline to continue behavioral studies in avians.

CONCLUSION

In conclusion, the rapid uptake times of ^{18}F-FDG both in the awake, behaving rat and the anesthetized chicken together with the rapid dynamics of rat and chicken behavior suggest that uptake times matched accurately with behavior for the same time periods will reduce random error in brain-behavior correlations. Furthermore, we have explored a new, dynamic-like ^{18}F-FDG injection protocol for use with the RatCAP scanner, which allowed us to repeatedly assess uptake during behavior across a 120 min scan. Using this method, we showed that most information in an ^{18}F-FDG scan is located where most of the uptake occurs, which, in turn, predicted changes in behavioral activity. Drug interventions or conditions that make behavior more predictable might increase the window under which PET-behavior correlations become observable. Future research will need to resolve the question whether group averages need to be the goal of RatCAP research or whether the statistics that we generate from time series in individual animals are a promising avenue that may help personalized medicine. It will also be of interest to analyze other behaviors for correlation with ^{18}F-FDG. This will require properly designed paradigms that increase mobility and are suitable for use with RatCAP tomography. While avian PET scanning is in its infancy, our previous work with starlings (Gold et al., 2016) and our current work with chickens provides impetus for comparative studies that in the long run could help determine brain function.

AUTHOR CONTRIBUTIONS

MG, MN, PV, and DS designed the experiments. MG, MB, and DS ran the analyses and interpreted the data. MG, MN, PV, and DS wrote the manuscript. MG, MN, MB, PV, and DS approved of the manuscript.

FUNDING

MG was supported by ExxonMobil, the Jurassic Foundation, the Paleontological Society, the Richard Gilder Graduate School, and the American Museum for Natural History. MN was supported by the American Museum for Natural History Division of Paleontology, the Macaulay Family Endowment, the Newt and Calista Gingrich Foundations, and NSF DEB-1457181. Additional support was provided by NSF DEB-1311790 (MN and MG). Funding for RatCAP research was provided by NIH R21DA029245 to DS. DS was supported by NIH R21DA029245, RF SUNY, and Yeditepe University. PV was supported by NIH R21DA029245 and DOE OBER. This research was carried out at Brookhaven National Laboratory under contract DE-AC02-98CH10886 with the U.S. Department of Energy.

ACKNOWLEDGMENTS

We would like to thank the Richard Gilder Graduate School, American Museum of Natural History, Brookhaven National Laboratory, J. S. Fowler and the Brookhaven radiochemistry, and the Brookhaven Laboratory Animal Facility.

REFERENCES

Albin, R. L., Young, A. B., and Penney, J. B. (1989). The functional anatomy of basal ganglia disorders. *Trends Neurosci.* 12, 366–375. doi: 10.1016/0166-2236(89)90074-X

Alexoff, D. L., Vaska, P., Marsteller, D., Gerasimov, T., Li, J., Logan, J., et al. (2003). Reproducibility of 11C-raclopride binding in the rat brain measured with the microPET R4: effects of scatter correction and tracer specific activity. *J. Nucl. Med.* 44, 815–822.

Babbini, M., and Davis, W. M. (1972). Time-dose relationships for locomotor activity effects of morphine after acute or repeated treatment. *Br. J. Pharmacol.* 46, 213–224. doi: 10.1111/j.1476-5381.1972.tb06866.x

Balanoff, A. M., Beyer, G. S., Rowe, T. B., and Norell, M. A. (2013). Evolutionary origins of the avian brain. *Nature* 501, 93–96. doi: 10.1038/nature12424

Belo, P. S., Romsos, D. R., and Leveille, G. A. (1976). Blood metabolites and glucose metabolism in the fed and fasted chicken. *J. Nutr.* 106, 1135–1143.

Berlyne, D. E. (1955). The arousal and satiation of perceptual curiosity in the rat. *J. Comp. Physio. Psych.* 48, 238–246. doi: 10.1037/h0042968

Berlyne, D. E. (1966). Curiosity and exploration. *Science* 153, 25–33. doi: 10.1126/science.153.3731.25

Berridge, K. C., and Whishaw, I. Q. (1992). Cortex, striatum and cerebellum: control of serial order in a grooming sequence. *Exp. Brain Res.* 90, 275–290. doi: 10.1007/BF00227239

Cross, D. C., Marzluff, J. M., Palmquist, I., Minoshima, S., Shimizu, T., and Miyaoka, R. (2013). Distinct neural circuits underlie assessment of a diversity of natural dangers by American crows. *Proc. Biol. Sci.* 280:20131046. doi: 10.1098/rspb.2013.1046

Di Chiara, G., and Imperato, A. (1988). Opposite effects of mu and kappa opiate agonists on dopamine release in the nucleus accumbens and in the dorsal caudate of freely moving rats. *J. Pharmacol. Exp. Ther.* 244, 1067–1080.

Doyon, J., Penhune, V., and Ungerleider, L. G. (2003). Distinct contribution of the cortico-striatal and cortico-cerebellar systems to motor skill learning. *Neuropsychologia* 41, 252–262. doi: 10.1016/S0028-3932(02)00158-6

Fair, J., Paul, E., and Jones, J. (eds.). (2010). *Guidelines to the Use of Wild Birds in Research*. Washington, DC: Ornithological Council.

Fowler, A. (2007). "Fluid therapy in wildlife," in *National Wildlife Rehabilitation Conference Proceedings* (Fremantle, WA).

Gallagher, B. M., Fowler, J. S., Gutterson, N. I., MacGregor, R. R., Wan, C.-N., and Wolf, A. P. (1978). Metabolic trapping as a principle of radiopharmaceutical design: some factors responsible for the biodistribution of [^{18}F] 2-deoxy-2-fluoro-D-glucose. *J. Nucl. Med.* 19, 1154–1161.

Gerfen, C. R., Engber, T. M., Mahan, L. C., Susel, Z., Chase, T. N., Monsma, F. J., et al. (1990). D1 and D2 dopamine receptor-regulated gene expression of striatonigral and striatopallidal neurons. *Science* 250, 1429–1432. doi: 10.1126/science.2147780

Gettys, G. C., Liu, F., Kimlin, E., Baghdoyan, H. A., and Lydic, R. (2013). Adenosine A1 receptors in mouse pontine reticular formation depress breathing, increase anesthesia recovery time, and decrease acetylcholine release. *Anesthesiology* 118, 327–336. doi: 10.1097/ALN.0b013e31827d413e

Glazier, D. S. (2005). Beyond the '3/4-power law': variation in the intra- and interspecific scaling of metabolic rate in animals. *Biol. Rev. Camb. Philos. Soc.* 80, 611–662. doi: 10.1017/S1464793105006834

Gold, M. E. L., Schulz, D., Budassi, M., Gignac, P. M., Vaska, P., and Norell, M. A. (2016). Flying starlings, PET, and the evolution of volant dinosaurs. *Curr. Biol.* 26, R265–R267. doi: 10.1016/j.cub.2016.02.025

Huston, J. P., Haas, H. L., Boix, F., Pfister, M., Decking, U., Schrader, J., et al. (1996). Extracellular adenosine levels in neostriatum and hippocampus during rest and activity periods of rats. *Neuroscience* 73, 99–107. doi: 10.1016/0306-4522(96)00021-8

Jang, D.-P., Lee, S.-H., Lee, S.-Y., Park, C.-W., Cho, Z.-H., and Kim, Y.-B. (2009). Neural responses of rats in the forced swimming test: [F-18]FDG microPET study. *Behav. Brain Res.* 203, 43–47. doi: 10.1016/j.bbr.2009.04.020

Jones, M. P., Morandi, F., Wall, J. S., Long, M. J., Stuckey, A. C., and LeBlanc, A. K. (2013). Distribution of 2-deoxy-2-fluoro-D-glucose in the coelom of healthy bald eagles (*Haliaeetus leucocephalus*). *Am. J. Vet. Res.* 74, 426–432. doi: 10.2460/ajvr.74.3.426

Kishore, A., Meunier, S., and Popa, T. (2014). Cerebellar influence on motor cortex plasticity: behavioral implications for Parkinson's disease. *Front. Neurol.* 5:68. doi: 10.3389/fneur.2014.00068

Kita, H., and Kitai, S. T. (1988). Glutamate decarboxylate immunoreactive neurons in rat neostriatum: their morphological types and populations. *Brain Res.* 447, 346–352. doi: 10.1016/0006-8993(88)91138-9

Kornblum, H. I., Araujo, D. M., Annala, A. J., Tatsukawa, K. J., Phelps, M. E., and Cherry, S. R. (2000). *In vivo* imaging of neuronal activation and plasticity in the rat brain by high resolution positron emission tomography (microPET). *Nature Biotech.* 18, 655–660. doi: 10.1038/76509

LeDoux, J. E. (1993). Emotional memory systems in the brain. *Behav. Brain Res.* 58, 69–79. doi: 10.1016/0166-4328(93)90091-4

Leipold, R. (1987). Injection technics for birds. *Tierarztl. Prax.* 15, 377–380.

Maher, F. (1995). Immunolocalization of GLUT1 and GLUT3 glucose transporters in primary cultured neurons and glia. *J. Neurosci. Res.* 42, 459–469. doi: 10.1002/jnr.490420404

Marzluff, J. M., Miyaoka, R., Minoshima, S., and Cross, D. J. (2012). Brain imaging reveals neuronal circuitry underlying the crow's perception of human faces. *Proc. Natl. Acad. Sci. U.S.A.* 109, 15912–15917. doi: 10.1073/pnas.1206109109

McMurray, R. G., Soares, J., Caspersen, C. J., and McCurdy, T. (2014). Examining variations of resting metabolic rate of adults: a public health perspective. *Med. Sci. Sports Exerc.* 46, 1352–1358. doi: 10.1249/MSS.0000000000000232

Mirrione, M. M., Schiffer, W. K., Fowler, J. S., Alexoff, D. L., Dewey, S. L., and Tsirka, S. E. (2007). A novel approach for imaging brain-behaviour relationships in mice reveals unexpected metabolic patterns during seizures in the absence of tissue plasminogen activator. *Neuroimage* 15, 34–42. doi: 10.1016/j.neuroimage.2007.06.032

Morris, R. G. M., Garrud, P., Rawlins, J. N. P., and O'Keefe, J. (1982). Place navigation impaired in rats with hippocampal lesions. *Nature* 297, 681–683.

Mueller, P., and Diamond, J. (2001). Metabolic rate and environmental productivity: well-provisioned animals evolved to run fast and idle fast. *Proc. Natl. Acad. Sci. U.S.A.* 98, 12550–12554. doi: 10.1073/pnas.221456698

Myers, R. (2001). The biological application of small animal PET imaging. *Nuc. Med. Biol.* 28, 585–593. doi: 10.1016/S0969-8051(01)00213-X

Myers, R., and Hume, S. (2002). Small animal PET. *Eur. Neuropsychopharm.* 12, 545–555. doi: 10.1016/S0924-977X(02)00103-7

Paxinos, G., and Watson, C. (2007). *The Rat Brain in Stereotaxic Coordinates*. Amsterdam: Elsevier/Academic Press.

Prum, R. O., and Dyck, J. (2003). A hierarchical model of plumage: morphology development, and evolution. *J. Exp. Zool. B Mol. Dev. Evol.* 298, 73–90. doi: 10.1002/jez.b.27

Raichlen, D. A., Gordon, A. D., Muchlinski, M. N., and Snodgrass, J. J. (2010). Causes and significance of variation in mammalian basal metabolism. *J. Comp. Physiol. B.* 180, 301–311. doi: 10.1007/s00360-009-0399-4

Reivich, M., Kuhl, D., Wolf, A., Greenberg, J., Phelps, M., Ido, T., et al. (1979). The [^{18}F]Fluorodeoxyglucose method for the measurement of local cerebral glucose utilization in man. *Circ. Res.* 44, 127–137. doi: 10.1161/01.RES.44.1.127

Sanes, J. N., and Donoghue, J. P. (2000). Plasticity and primary motor cortex. *Annu. Rev. Neurosci.* 23, 393–415. doi: 10.1146/annurev.neuro.23.1.393

Schadrack, J., Willoch, F., Platzer, S., Bartenstein, P., Mahal, B., Dworzak, D., et al. (1999). Opioid receptors in the human cerebellum: evidence from [11C]diprenorphine PET, mRNA expression and autoradiography. *Neuroreport* 10, 619–624. doi: 10.1097/00001756-199902250-00032

Schiffer, W. K., Mirrione, M. M., and Dewey, S. L. (2007). Optimizing experimental protocols for quantitative behavioral imaging with ^{18}F-FDG in rodents. *J. Nucl. Med.* 48, 277–287.

Schmidt, K., Lucignani, G., and Sokoloff, L. (1996). Fluorine-18-Fluorodeoxyglucose PET to determine regional cerebral glucose utilization: a re-examination. *J. Nucl. Med.* 37, 394–399.

Schulz, D., Southekal, S., Junnarkar, S. S., Pratte, J. F., Purschke, M. L., Stoll, S. P., et al. (2011). Simultaneous assessment of rodent behavior and neurochemistry using a miniature positron emission tomograph. *Nat. Methods.* 8, 347–352. doi: 10.1038/nmeth.1582

Shackman, A. J., Fox, A. S., Oler, J. A., Shelton, S. E., Davidson, R. J., and Kalin, N. H. (2013). Neural mechanisms underlying heterogeneity in the presentation of anxious temperament. *Proc. Natl. Acad. Sci. U.S.A.* 110, 6145–6150. doi: 10.1073/pnas.1214364110

Sokoloff, L., Reivich, M., Kennedy, C., Des Rosiers, M. H., Patlak, C. S., Pettigrew, K. D., et al. (1977). The [14C]deoxyglucose method for the measurement of local cerebral glucose utilization: theory, procedure, and normal values in the conscious and anesthetized albino rat. *J. Neurochem.* 28, 897–916. doi: 10.1111/j.1471-4159.1977.tb10649.x

Southekal, S., Purschke, M. L., Schlyer, D. J., and Vaska, P. (2011). Quantitative PET imaging using a comprehensive Monte Carlo system model. *IEEE Trans. Nucl. Sci.* 58, 2286–2295. doi: 10.1109/TNS.2011.2160094

Souza, M. J., Wall, J. S., Stuckey, A., and Daniel, G. B. (2010). Static and dynamic 18-FDG-PET in normal Hispaniolan Amazon Parrots (*Amazona ventralis*). *Vet. Radiol. Ultrasound.* 52, 340–344. doi: 10.1111/j.1740-8261.2010.01793.x

Stevens, L. (1996). "Carbohydrate and intermediary metabolism," in *Avian Biochemistry and Molecular Biology*, ed L. Stevens (Cambridge: Cambridge University Press), 29–45.

Thompson, S. J., Millecamps, M., Aliaga, A., Seminowicz, D. A., Low, L. A., Bedell, B. J., et al. (2014). Metabolic brain activity suggestive of persistent pain in a rat model of neuropathic pain. *Neuroimage* 91, 344–352. doi: 10.1016/j.neuroimage.2014.01.020

Wagner, G. P., and Gauthier, J. A. (1999). 1, 2, 3= 2, 3, 4: a solution to the problem of the homology of the digits in the avian hand. *Proc. Natl. Acad. Sci. U.S.A.* 96, 5111–5116.

Wahl, R. L., Kaminski, M. S., Ethier, S. P., and Hutchins, G. D. (1990). The potential of 2-deoxy-2[^{18}F]fluoro-D-glucose (FDG) for the detection of tumor involvement in lymph nodes. *J. Nucl. Med.* 31, 1831–1835.

Wang, H., Moriwaki, A., Wang, J. B., Uhl, G. R., and Pickel, V. M. (1996). Ultrastructural immunocytochemical localization of mu opioid receptors and Leu5-enkephalin in the patch compartment of the rat caudate-putamen nucleus. *J. Comp. Neurol.* 375, 659–674. doi: 10.1002/(SICI)1096-9861(19961125)375:4<659::AID-CNE7>3.0.CO;2-0

Wang, H., Moriwaki, A., Wang, J. B., Uhl, G. R., and Pickel, V. M. (1997). Ultrastructural immunocytochemical localization of mu-opioid receptors in dendritic targets of dopaminergic terminals in the rat caudate-putamen nucleus. *Neuroscience* 81, 757–771. doi: 10.1016/S0306-4522(97)00253-4

Welten, M. C. M., Verveek, F. J., Meijer, A. H., and Richardson, M. K. (2005). Gene expression and digit homology in the chicken embryo wing. *Evol. Dev.* 7, 18–28. doi: 10.1111/j.1525-142X.2005.05003.x

Wichmann, T., and DeLong, M. R. (2010). "Deep-brain stimulation for neurologic and psychiatric disorders," in *Handbook of Basal Ganglia Structure and Function*, eds H. Steiner and K. Y. Tseng (Amsterdam: Elsevier/Academic Press), 659–681.

Conflict of Interest Statement: The authors declare that the research was conducted in the absence of any commercial or financial relationships that could be construed as a potential conflict of interest.